

Electron backscattered diffraction method in the analysis of deformed steel structures

Elena Pashinska, Victor Varyukhin, Anatoliy Zavdoveev, Valeriy Burkhovetskii, Valentina Glazunova*

Donetsk Institute of Physics and Engineering, Ukrainian Academy of Sciences,

83114, R. Luxemburg str. 72, Donetsk, Ukraine

(Dated: March 3, 2013)

The structure of low-carbon steel after twist extrusion is tested with using electron backscattered diffraction. It has been shown that warm twist extrusion results in grain refinement with conservation of a substantial part of high-angle boundaries, smearing of the texture, more homogeneous distribution of grains and development of the dynamic recrystallization processes.

PACS numbers: 61.05.-a, 61.05.J-

I. INTRODUCTION

It is well known that severe plastic deformation allows obtaining of materials combining high strength with plasticity. One of such methods is twist extrusion (TE) that is extruding of a prismatic billet through the die with twist channel. Channel geometry enables the deformed billet to preserve the size and the form identical to the initial state. The maximum accumulated deformation per one pass is $e = tg\beta$ (β is the descent angle of the twist line) [1, 2]. Earlier, we analyzed the effect of TE on the redistribution of alloying elements in low-carbon construction steel and formulated general conceptions of morphological structure changes [3]. To obtain more detailed description of structure changes in low-carbon steels under TE, the method of automatic analysis of images of electron backscattering diffraction (EBSD) was used here [4].

II. MATERIAL AND METHOD OF EXPERIMENT

As investigated material was low-carbon steel 20G2C of the following composition, mass in percent: 0,24C; 1,66Mn; 1,2Si; 0,14Cr; 0,24Ni; 0,01Al; 0,04S. The samples were obtained by warm forging (400°C) and succeeding milling down to cross-section of 2439mm. Then the samples were annealed at 920°C for 1 hour and cooled in air. The extrusion was carried out with hydraulic press performing three passes at $P_{max} \approx 200MPa$ and backpressure of 100Pa. Before the first pass, the sample was heated up to 850 °C; before the second and the third pass, the heating was done up to 400 °C; the temperature of the equipment was 320 °C in all the cases. The total accumulated deformation was $e = 6$.

Electron scanning microscope JSM-6490LV (JEOL, Japan) with special holder for bulk samples of 10×10×15 mm in size was used for EBSD analysis of structure changes. The principle of the analysis is well known; electron beam scans the selected surface of the sample and

Kikuchi images consisting of Kikuchi bands are plotted for every point. Every band is associated with a definite group of crystal planes. Using software of *HKLC Chanel5*, we established the position of each Kikuchi band, compared it with the theoretical data and calculated three-dimensional crystallographic orientation of the lattice. The obtained three-dimensional information was used for reconstruction of the microstructure.

To accumulate a representative sample, we had to analyze at least 1500 grains on the specimen. Thus, the following procedure was applied: magnification of $\times(600700)$ was used, scanning area was $150 \times 100 \mu$, scanning step was 500nm (at least 10 measuring points per a grain). The degree of indicating was at least 80 percent, the required result was not achieved at a lower value. The method allowed both qualitative analysis by mapping and qualitative analysis using statistical data. Besides, texture analysis was done. For more detailed structure reconstruction, the threshold of noise misorientation was established at 5°. At lower threshold, sub-grain boundaries would be taken into account and the analysis of EBSD-maps would be complicated. Nevertheless, when analyzing distributions of grains and sub-grains and drawing pole figures, the whole data set was accounted including misorientations below the threshold of 5°.

III. RESULTS AND DISCUSSION

A. Microstructure reconstruction, qualitative analysis

For the visualization of grain morphology, contrast maps were created where grains were depicted in gray tones and grain boundaries were represented by black lines (Fig. 1, a, b). Contrast maps are similar to the structure images obtained with the optical microscope. The maps of small-angle and high-angle boundaries were drawn for detailed analysis of the grain boundaries (Fig. 1, c, d). Boundaries with the misorientation angle less than 15° are colored in green and those above the given threshold are colored in black.

We have obtained also the maps characterizing the part of strained (deformed) and unstrained (recrystal-

* zavdoveev@fti.dn.ua

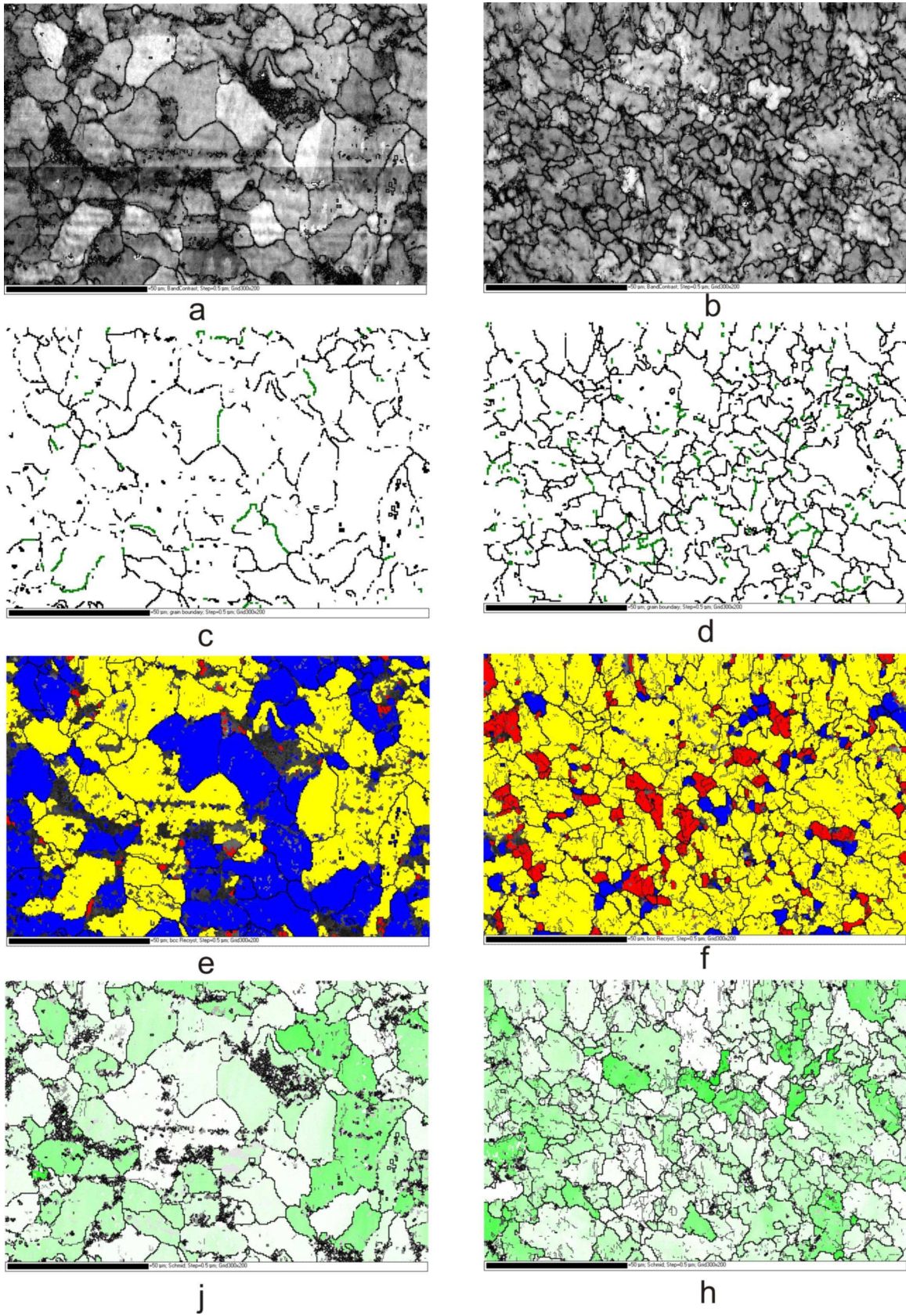


FIG. 1. Reconstruction of the microstructure of low-carbon steel in the initial state (a, c, e, g) and after torsional extrusion (b, d, f, h) by EBSD maps: a,b are contrast maps; c,d are maps of grain boundary misorientation; e,f are maps of re-crystallization; g,h are maps of Schmid's factor

lized) grains (Fig. 1, e, f) in steel after TE: unstrained recrystallized grains are marked by blue color, polygonized grains are marked by yellow color and deformed grains are red (These maps have been built only for bcc-iron. Beside bcc-iron, steel contains some fcc-iron and cementite. According to EBSD data, the initial composition was as follows: 78,5 percent of bcc iron, 1,5 percent of fcc iron and 20 percent of Fe_3C ; the composition in the deformed state was: 92 percent of bcc iron, 2 percent of fcc iron and 6 percent of Fe_3C). The basic idea of these maps is that if there are no misorientations in the neighbor pairs of the analyzed points within a grain, the grain is identified as an unstrained recrystallized one. In the case when misorientations between two neighbor subgrains exceed 2° , the grain is polygonized and if they are above this value, the grain is a deformed one.

Homogeneity of deformation was analyzed with the use of Schmid's maps. The slip system $\langle 111 \rangle (110)$ was selected as the most informative one in bcc iron. Schmid's factor is evaluated as [4]: $m = \cos\lambda \cdot \cos\chi$, where λ is the angle between the slip direction and the deformation axis, χ is the angle between the normal to the slip plane and the deformation axis. The maximum value of Schmid's factor is achieved at $\chi = \lambda = 45^\circ$. A macroscopic shift occurs when the shear strain in the given slip system reaches the maximum value τ_0 , that is called the critical shear strain. Shear strain τ is related to Schmid's factor as $\tau = \tau_0 \cdot m$. Thus, Schmid's maps show, what grain will be deformed earlier under uniaxial loading (these grains are colored in light, Fig. 1, j, h).

Correlation of EBSD-maps of different types is explicitly seen. All of them demonstrate grain refinement from 15μ to 5μ after TE and substantial part of high-angle boundaries. This fact is confirmed by data of optical and electron scanning microscopy.

After warm deformation by TE, recrystallized ferrite grains are detected in the material (Fig. 1 e, f). They are located mostly near high-angle boundaries but never within large grains. Similar location of recrystallized volume near grain boundaries was observed in the deformed nickel alloy [5]; a suggestion was made that recrystallization nuclei are formed in the most distorted areas of the lattice, i.e. at high-angle grain boundaries.

Nevertheless, small recrystallized grains were found within a large polygonized grain. In this case, we suppose that they were formed from a few adjoining subgrains by defect flow toward the polygonized grain boundary inside the grain. The result was the reduction of defect density in the subgrain and increased misorientation of the boundary up to the high-angle one (Fig.1 f). This fact means that two processes (dynamical polygonization and dynamical recrystallization) progress simultaneously. These processes can occur jointly or by turns. Thus, the analysis of EBSD maps gives evidences that the structure of the tested steel consists of fragmented, polygonized and recrystallized grains.

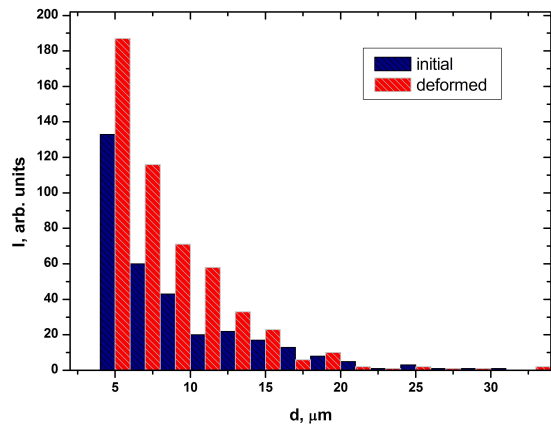


FIG. 2. Frequency distribution of grains by size

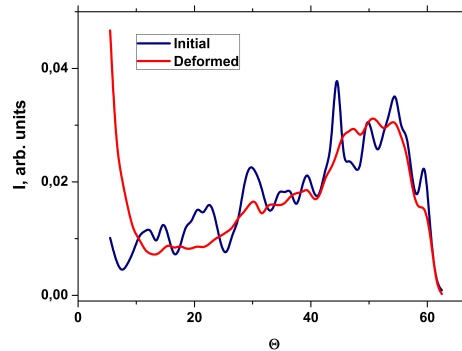


FIG. 3. Frequency distribution of misorientation angles of grain boundaries

B. Quantitative analysis

On the basis of statistical analysis of the data of EBSD maps, graphs of the frequency distribution of the grain size and misorientation angles were constructed. It follows from Fig.2 that the metal structure in the initial state was characterized by bimodal grain distribution with the maximums at 13μ and 5μ , i.e. by explicit difference in the grain size. After TE, the distribution became more homogeneous with the maximum at 5μ confirmed by EBSD-maps (see. Fig. 1, a, b).

According to the distribution of grain boundary misorientation angles (Fig. 3), the specific part of high-angle boundaries in the initial material was about 91 percent. This parameter was retained at high level (84 percent) in the deformed material, too. The formation of small-angle boundaries could be explained by specific features of the material. For instance, in copper under TE, formation of small-angle boundaries prevails at the initial deformation stages, but their amount is reduced at developed deformation [6]. We can suggest that high-angle grain boundaries will dominate in steel at accumulation

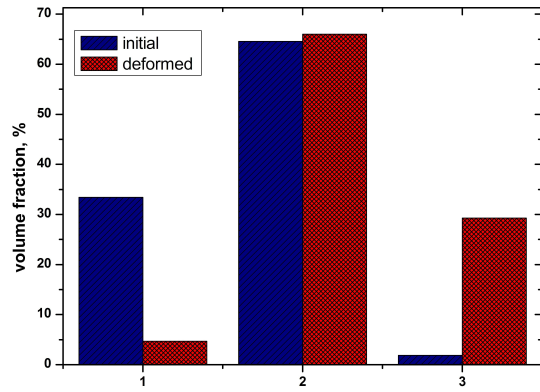


FIG. 4. Component distribution of steel microstructure: 1 recrystallized grains, 2 polygonized grains; 3 deformed grains

of higher deformation degree.

Fig. 4 illustrates parts of different grains depending on the state of the material. The data were obtained by numerical processing of EBSD maps (Fig.1 e,f). So, we can make a conclusion that the content of recrystallized grains in the initial state of the sample was 33,4 percent, and this amount was reduced to 4,7 percent after the deformation. As the deformation of the sample in the course of processing is substantial, all grains are deformed with succeeding passing the stages of defect density accumulation, fragmentation, dynamical polygonization and dynamical re-crystallization. Thus, occurrence of 4,7 percent of recrystallized areas can be explained by active relaxation processes. The effect of dynamical recrystallization of steel at severe plastic deformation was observed in a number of experiments: for example, at ECAP [7], HPT[8].

C. Texture analysis

As distinct from traditional X-ray methods used for the tests of large areas of a specimen, EBSD method allows detailed analysis of texture evolution in the selected zones. Figs. 5 and 6 demonstrate pole figures registered in the areas of about $15000\mu^2$ in size. The analysis of inverse pole figures gives information not only about the presence of the texture in the sample but also about the mechanisms involved in the course of the processing. In

the case of one of another prevailing pole density, we can make conclusions about the dominating relaxation mechanism (intragrain or intergrain sliding), and texture evolution can be related to the change of deformation mechanisms or development of dynamical recrystallization [9]. If the maximum pole density is located near $\langle 111 \rangle$ and $\langle 110 \rangle$ orientation, the mechanisms of twinning progressed actively within the sample [10]. If the intensity of the outlet of normal lines is reduced, (the texture is smearing) and the distribution becomes more homogeneous as in the case considered above (Fig. 5), we can say about activated non-crystallographic mechanisms of plastic deformation.

Texture analysis cannot be accomplished without the analysis of direct pole figures characterizing the density of the outlet of normal lines of definite crystallographic planes (here these are $\langle 111 \rangle$, $\langle 110 \rangle$, $\langle 100 \rangle$ planes). The direct pole figures confirm the fact that axial features of the texture are reduced in the tested steel after TE, being weakly expressed in general. Two factors can be associated with this phenomenon, these are peculiarities of the deformation scheme (transversal flow of metal) and relaxation processes. Accidentally arranged sharp texture maximums present in pole figures can indicate to the appearance of recrystallized grains [9]. Because of possible ambiguity, this effect requires additional investigations.

IV. SHORT CONCLUSION

The use of EBSD method has revealed effect of twist extrusion of the structure of low-carbon construction steel. Besides grain refinement and texture smearing, such treatment results in more homogeneous structure with a substantial part of high-angle boundaries. This fact is explained by peculiarities of the deformation scheme at twist extrusion and evolution of relaxation processes.

ACKNOWLEDGMENTS

The authors are very grateful to Prof. S.V. Dobatkin for the material granted for the experiments, to Dr. B.M. Efros for productive discussion and to providing engineer B.. Stebletsov for the aid in construction of the sample holder.

-
- [1] Ya. Beygelzimer V. Varyukhin D. Orlovand S. Sinkov, *Twist extrusion process of deformation accumulation* (TEAN, Donetsk, 2003).
 [2] Y. Beygelzimer, V. Varyukhin, S. Synkov, D. Orlov, Mat. Sci. Eng. **A503**, 14, (2009).

- [3] E. Pashinska S. Dobatkin V. Varyukhin Ya. Beygelzimerand A. Zavdoveev, *Warm severe plastic deformation of building steel: structure and properties* (12 European Congress on Advanced Materials and Processes Euromat, 12-15 September 2011, Montpellier, France, ref2707 2011).

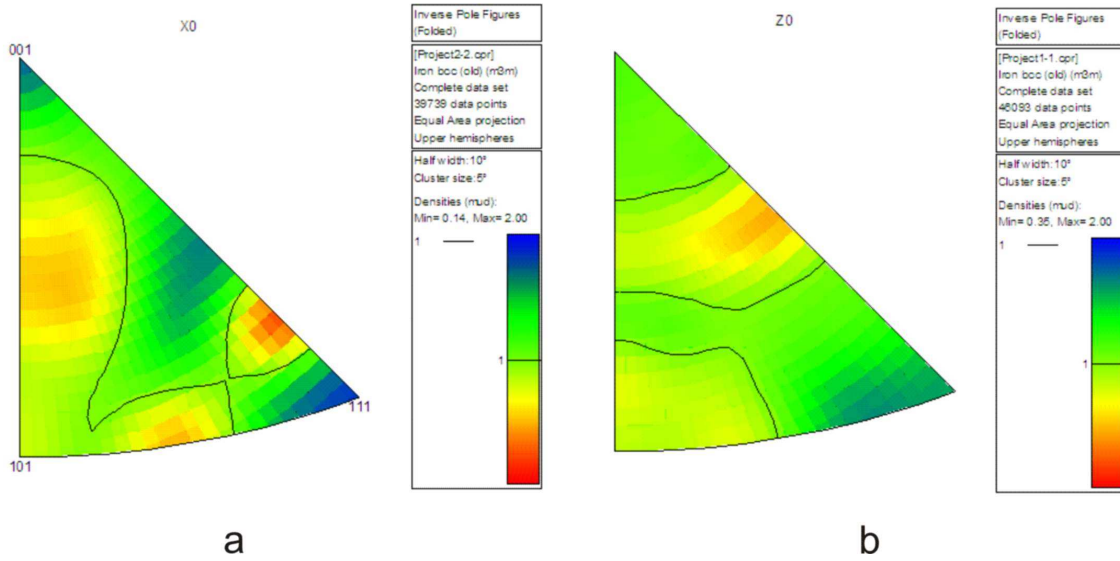


FIG. 5. Inverse pole figures of steel: initial state (a) deformed state (b)

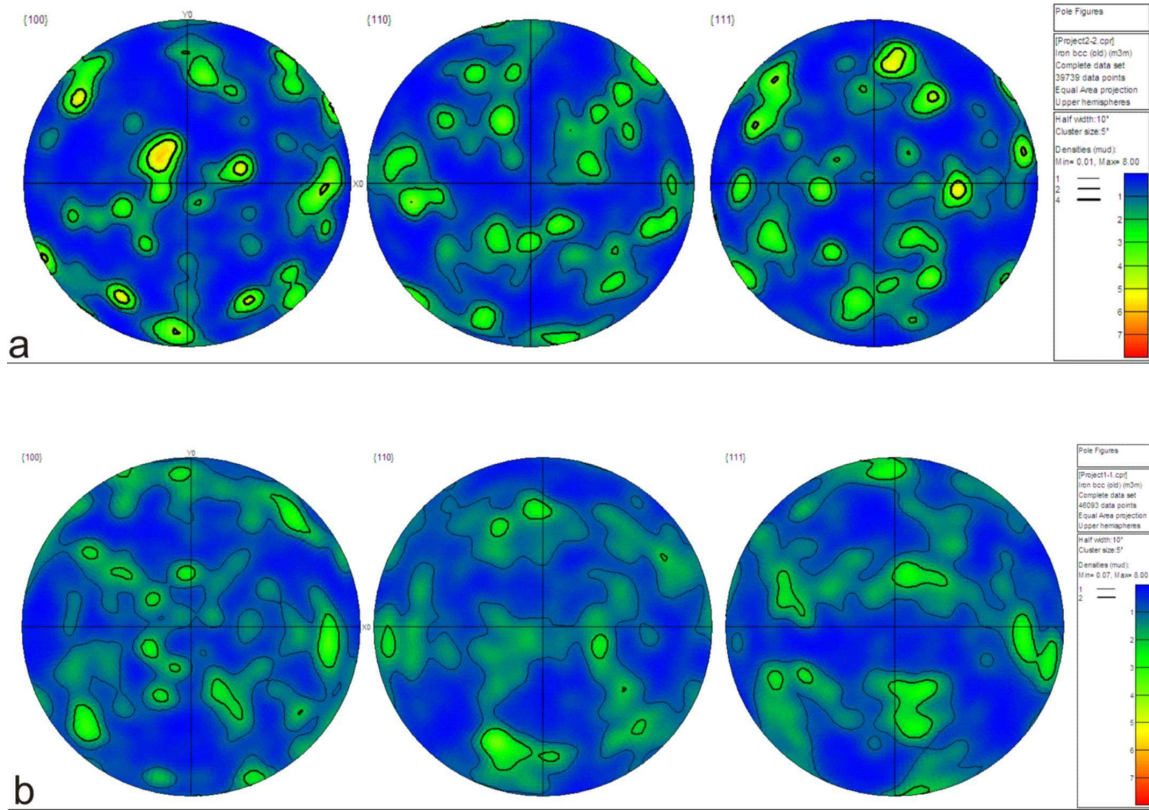


FIG. 6. Pole figures of steel: initial state (a) deformed state (b)

- [4] R. Larsen, *Using EBSD to evaluate the anisotropic behavior and martensite formation in austenitic stainless steel* (Proc. EBSD Users Meeting. 2006, Hindsgavi Castle, Denmark, ref2707 2006).
- [5] S. Mitsche C. Sommitsch P. Polt, *EBSD Analysis of the recrystallization of the Nickel based alloy 80A during hot forming* (Praktischen Metallographie. 2006., Sonderbnde, 43 2006).
- [6] V. Varyukhin E. Pashinska V. Tkachenko M. Mishlyaev, *Evolution of structure and properties of FRTP Cu at twist extrusion and further thermo deformation treatment* (HP 2010, Sudak, Crimea, Ukraine, 143 2010).
- [7] S. Dobatkin P. Odessky and S. Shagalina, *Mat. Sci. Forum.* **584-586**, 623 (2008).

- [8] A. Glezer, and L. Metlov, Solid State Physics **52**, 1090 (2010).
- [9] M. Mishlyaev, S. Mironov, Yu. Perlovich, and M. Isaenkova, Report of Academy of Science **430**, 5, 618 (2010).
- [10] S. Dancette, L. Delannay, K. Renard, M. Melchior, and P. Jacques, Acta Materialia **60**, 5, 2135 (2012).